



HAL
open science

Universal scaling of the formation factor in clays: Example from the Nankai Trough

Hugh Daigle, Behzad Ghanbarian, Pierre Henry, Marianne Conin

► To cite this version:

Hugh Daigle, Behzad Ghanbarian, Pierre Henry, Marianne Conin. Universal scaling of the formation factor in clays: Example from the Nankai Trough. *Journal of Geophysical Research: Solid Earth*, 2015, 120 (11), pp.7361 - 7375. 10.1002/2015JB012262 . hal-01784106

HAL Id: hal-01784106

<https://hal.science/hal-01784106>

Submitted on 13 Dec 2021

HAL is a multi-disciplinary open access archive for the deposit and dissemination of scientific research documents, whether they are published or not. The documents may come from teaching and research institutions in France or abroad, or from public or private research centers.

L'archive ouverte pluridisciplinaire **HAL**, est destinée au dépôt et à la diffusion de documents scientifiques de niveau recherche, publiés ou non, émanant des établissements d'enseignement et de recherche français ou étrangers, des laboratoires publics ou privés.

Copyright

RESEARCH ARTICLE

10.1002/2015JB012262

Key Points:

- Formation factor in clays follows universal scaling from percolation theory
- Percolating electrical current paths do not include clay-bound water
- Percolation scaling is valid over the entire range of observed porosities

Supporting Information:

- Tables S1–S6

Correspondence to:

H. Daigle,
daigle@austin.utexas.edu

Citation:

Daigle, H., B. Ghanbarian, P. Henry, and M. Conin (2015), Universal scaling of the formation factor in clays: Example from the Nankai Trough, *J. Geophys. Res. Solid Earth*, 120, 7361–7375, doi:10.1002/2015JB012262.

Received 5 JUN 2015

Accepted 26 OCT 2015

Accepted article online 27 OCT 2015

Published online 21 NOV 2015

Universal scaling of the formation factor in clays: Example from the Nankai Trough

Hugh Daigle¹, Behzad Ghanbarian¹, Pierre Henry², and Marianne Conin³

¹Department of Petroleum and Geosystems Engineering, University of Texas at Austin, Austin, Texas, USA, ²Centre Européen de Recherche et d'Enseignement des Géosciences de l'Environnement, Centre National de la Recherche Scientifique, Aix-en-Provence, France, ³University of Lorraine, Centre National de la Recherche Scientifique, Centre de Recherches sur la Géologie des Matières Premières Minérales et Energétiques, GeoRessources Laboratory, Nancy School of Mines, Nancy, France

Abstract Electrical conductivity is a fundamental characteristic describing how strongly a network opposes flow of electrical current. In fully water-saturated porous media the conductivity, represented by the formation factor, is mainly controlled by porosity, connectivity of the conducting phases, and the tortuosity of electrical current paths. Previous work has shown that universal scaling derived from percolation and effective medium theories accurately describes the relationship between formation factor and porosity when the percolation threshold is taken account, as well as the porosity value at which the scaling switches from percolation theory to effective medium theory. We determined the formation factor in clay-rich sediments based on cation exchange capacity measurements on samples from five scientific ocean drilling sites in the Nankai Trough. We then compared the results to predictions from universal scaling after determining the volume of clay-bound water and the percolation threshold. We found that the previously reported universal scaling relations hold in these clay-rich sediments once the corrections are made for the clay-bound water and that percolation scaling appears to be valid over the entire range of observed porosities, probably due to relatively broad pore size distributions or low pore system connectivity. Our results show that universal scaling can be applied to describe the porosity dependence of the formation factor in clay-rich sediments when appropriate corrections are made for the presence of clay-bound water.

1. Introduction

Electrical conductivity is an important porous medium property that may be used to determine porosity [e.g., Doll *et al.*, 1952] and permeability [Katz and Thompson, 1986; Skaggs, 2011], as well as the fraction of the pore space containing a nonconductive phase such as oil or gas [Archie, 1942]. Since downhole porosity measurements often involve the use of a radioactive source such as ¹³⁷Cs or a minitron [Ellis and Singer, 2007], the ability to determine porosity using other methods is an attractive way to minimize operational risk. In marine sediments, the phenomenological model of Archie [1942] is often used to determine porosity from electrical conductivity measurements [e.g., Kermabon *et al.*, 1969; Erickson and Jarrard, 1998]. The presence of clays in marine sediments complicates this analysis since electrical conductivity occurs both through the interconnected pore space as well as along clay grain surfaces, where a layer of weakly sorbed counterions forms to balance the negative surface charge of the clay grains [Waxman and Smits, 1968; Clavier *et al.*, 1984]. Accurate characterization of the electrical transport through this surface layer is essential for interpretation of conductivity measurements in clay-bearing sediments.

Electrical conductivity in disordered networks and porous media like semiconductors and rocks has been analyzed in the literature using both percolation theory and effective medium theory [Ambegaokar *et al.*, 1971; Kirkpatrick, 1971, 1973; Sen *et al.*, 1981; Ewing and Hunt, 2006; Hamamoto *et al.*, 2010; Ghanbarian *et al.*, 2014; Revil *et al.*, 2014; Hunt *et al.*, 2014a; Ghanbarian *et al.*, 2015a]. Percolation theory provides a robust theoretical framework to study flow and transport within disordered interconnected networks and porous media [Sahimi, 1994b, 2011]. In the percolation theory framework, above but near the percolation threshold transport properties (e.g., electrical conductivity and permeability) under fully saturated conditions follow a power law scaling with the difference between porosity ϕ and the percolation threshold ϕ_c [Sahimi *et al.*, 1984; Stauffer and Aharony, 1992; Sahimi, 1994b; Hunt *et al.*, 2014a]. The specific range of porosities that would be considered “near” the threshold has never been quantified. Nonetheless, analyses presented by

Ghanbarian-Alavijeh and Hunt [2012], Ghanbarian et al. [2013]. Ghanbarian and Hunt [2014], Hunt et al. [2014b], Ghanbarian et al. [2014], and Ghanbarian et al. [2015a] indicate that universal scaling from percolation theory is valid over a broader region above the percolation threshold in natural porous media. In the effective medium approach, a relatively disordered porous medium is replaced by a uniform one. Thus, local heterogeneities in the former cause local perturbations to the overall macroscopic transport properties of the latter. Within the effective medium theory framework, the macroscopic transport properties are expressed in terms of the transport properties of the local components by requiring that the volumetric average of the local perturbations is zero [Bruggeman, 1935; Kirkpatrick, 1973]. For a more comprehensive introduction to percolation and effective medium theories, see Sahimi [2003, 2011].

In general, the percolation theory universal scaling is theoretically valid when porosity is close to the percolation threshold, while the effective medium universal scaling is appropriate for porosity much greater than the percolation threshold. The porosity ϕ_x that separates the percolation and effective medium domains varies; the fraction of conducting bonds at which crossover occurs as reported by Kirkpatrick [1973] and Kiefer et al. [2009] for numerical simulations of resistor networks corresponds to a value of roughly 0.75, but values between 0.26 and 1 have been determined for natural porous media, and there is no evidence that there is a universal value [Ghanbarian et al., 2014]. The crossover porosity ϕ_x might be above the porosity of the medium (see, e.g., Ghanbarian et al. [2014]) or below it [Ghanbarian et al., 2015b]. Generally speaking, one should expect ϕ_x to be smaller than the total porosity in media with a narrow pore size distribution, and larger than the total porosity in media with a broad pore size distribution [Ghanbarian et al., 2015b].

For electrical conductivity, percolation and effective medium theories predict power law scaling with porosity but with different exponents. Ghanbarian et al. [2014] and Ghanbarian et al. [2015a] showed that conductivity scales with $(\phi - \phi_t)^2$ when porosity is close to the percolation threshold, and with $(\phi - \phi_t)$ when $\phi > \phi_x$. On the basis of this, Ghanbarian et al. [2014] showed that the formation factor F scaled with $(\phi - \phi_t)^{-2}$ for $\phi_t \leq \phi \leq \phi_x$, and with $(\phi - \phi_t)^{-1}$ when $\phi > \phi_x$. However, their work considered only experiments on rocks with negligible surface conductivity such that F could be expressed by σ_f/σ , where σ_f is the conductivity of the pore fluid and σ is the conductivity of the rock.

In rocks with significant amounts of clay, the porosity dependence of electrical conductivity under fully saturated conditions is more complicated. However, since F is strictly independent of surface conductivity, we show in what follows that it is still possible to express the formation factor as a function of porosity in rocks with non-zero surface conductivity as long as appropriate corrections are made for the surface conduction [e.g., Revil et al., 1998]. Therefore, by analogy we expect that the scaling of F with porosity proposed by Ghanbarian et al. [2014] should hold in clay-rich sediments as well. We present experimental measurements of marine clays collected from the Nankai Trough offshore Japan to confirm that the universal scaling derived from percolation and effective-medium theories holds even in porous media with significant surface conductivity contributions. We additionally show that quadratic scaling from percolation theory is applicable all the way to porosity of 1, which is likely a result of relatively broad pore size distributions or low pore system connectivity in these samples.

2. Background

The formation factor is defined as

$$\frac{1}{F} \equiv \frac{1}{V} \int_{V_p} |\mathbf{e}_b|^2 dV_p, \quad (1)$$

where \mathbf{e}_b is the normalized electric field in the interconnected pore space, defined as $-\nabla\psi/|\mathbf{E}|$, where \mathbf{E} is the macroscopic electric field and $\nabla\psi$ is the local electrical potential gradient; V is the volume of a representative elementary volume; and V_p is the interconnected pore volume [Johnson et al., 1986; Avellaneda and Torquato, 1991; Revil and Glover, 1997]. In sediments with nonzero grain surface conductivity, Revil et al. [1998] showed that for pore fluid pH between 5 and 8, F is related to the conductivity σ of the sediment by

$$\sigma = \frac{\sigma_f}{F} \left[1 - t_{(+)}^f + F\xi + \frac{1}{2} \left(t_{(+)}^f - \xi \right) \left(1 - \frac{\xi}{t_{(+)}^f} + \sqrt{\left(1 - \frac{\xi}{t_{(+)}^f} \right)^2 + \frac{4F\xi}{t_{(+)}^f}} \right) \right], \quad (2)$$

where $t_{(+)}^f$ is the Hittorf transport number of cations in the free electrolyte (pore fluid) and represents the fraction of the electrical current carried by these cations [Revil and Glover, 1997] and ξ is the ratio of surface

conductivity to fluid conductivity, known as the Dukhin number [Lyklema, 1993]. When ζ is small, indicating that cation migration occurs dominantly in the interconnected pore space rather than along clay grain surfaces, F may be determined from a Taylor series expansion of equation (2) [Bourlange et al., 2003] as

$$F = \frac{\sigma_f}{\sigma} \left[1 + 2\zeta \left(\frac{\sigma_f}{\sigma} - 1 \right) \right]. \quad (3)$$

The condition for small ζ is $\zeta/t_{(+)}^f \sim 1$ [Revil et al., 1998], and we caution that equation (3) is only valid when $\zeta \ll 1$. When $\zeta \rightarrow 0$, both equations (2) and (3) reduce to $F = \sigma_f/\sigma$, which is the original definition stated by Archie [1942].

2.1. Universal Scaling of the Formation Factor

Like other transport properties, in the absence of surface conductivity, electrical conductivity has been shown to follow percolation scaling when the porosity ϕ is close to, but greater than, the percolation threshold porosity ϕ_t [Stauffer and Aharony, 1992; Ghanbarian et al., 2014]:

$$\sigma(\phi) \propto (\phi - \phi_t)^t, \quad \phi_t \leq \phi \leq \phi_x, \quad (4)$$

where t is a scaling exponent. In three dimensions, if the pore size distribution is not too broad, a universal value of $t=2$ is expected [Gingold and Lobb, 1990; Stauffer and Aharony, 1992; Clerc et al., 2000], which means that the exponent t in equation (4) is invariant from system to system [Hunt et al., 2014a]. The value $t=2$ accounts for effects of both tortuosity and connectivity of the pore system in the pore volume in excess of the percolation threshold [Ghanbarian et al., 2014]. Values of $t > 2$ have been shown to occur in cases where the pore size distribution is broad; for example, Halperin et al. [1985] showed that $t \approx 2.5$ in a three-dimensional “Swiss-cheese” model in which nonconducting, spherical holes are randomly placed in a conducting medium. On the other hand, Sahimi and his coworkers [Sahimi, 1994a; Sahimi and Mukhopadhyay, 1996; Knackstedt et al., 2001] have demonstrated the one should expect $t < 2$ in media with long-range correlation. At the scale of laboratory samples, the appearance of universal scaling from percolation theory does not necessarily indicate universal scaling at the scale of borehole measurements, since laboratory samples are typically much smaller than the correlation length [e.g., Sahimi and Mukhopadhyay, 1996].

When $\phi \rightarrow 1$, the scaling given by equation (4) with $t=2$ may not be valid, and the electrical conductivity in the absence of surface conduction can be described from effective medium theory [Kirkpatrick, 1973; Sahimi, 1994b; Kennedy and Herrick, 2012; Ghanbarian et al., 2014]. Various nonlinear relationships between electrical conductivity and porosity or bond occupancy have been derived from effective medium theory [e.g., Turban, 1978; Sen et al., 1981; Mendelson and Cohen, 1982; Sali and Bergman, 1997; Torquato and Hyun, 2001], while Kirkpatrick [1973] and Sahimi et al. [1984] among others have shown that a simple linear relationship performs adequately in disordered media:

$$\frac{\sigma(\phi)}{\sigma_f} \approx \frac{\phi - \phi_t}{1 - \phi_t}. \quad (5)$$

The “approximately equal to” sign in equation (5) refers to the approximation of $2/Z$ as ϕ_t (where Z is the average coordination number) [e.g., Ghanbarian et al., 2014].

Equations (4) and (5) may be combined to express σ in terms of porosity in water-saturated rocks in the absence of surface conductivity by specifying that σ predicted by equation (4) must be equal to that predicted by equation (5) at some crossover porosity ϕ_x [e.g., Ghanbarian et al., 2014]:

$$\frac{\sigma(\phi)}{\sigma_f} = \begin{cases} \frac{1 - \phi_t (\phi - \phi_t)^2}{\phi_x - \phi_t (1 - \phi_t)}, & \phi_t < \phi < \phi_x \\ \frac{\phi - \phi_t}{1 - \phi_t}, & \phi_x < \phi < 1 \end{cases}, \quad (6)$$

where ϕ_x is a crossover porosity value above which the quadratic scaling from percolation theory scaling switches to linear scaling predicted from effective medium theory. We assume that the threshold porosity

ϕ_t corresponds to the ineffective porosity, that is porosity that does not contribute to flow through the pore space. The formation factor is obtained by taking the inverse of equation (6) and simplifying:

$$F = \begin{cases} \frac{(1 - \phi_t)(\phi_x - \phi_t)}{(\phi - \phi_t)^2}, & \phi_t < \phi < \phi_x \\ \frac{1 - \phi_t}{\phi - \phi_t}, & \phi_x < \phi < 1 \end{cases} \quad (7)$$

Ghanbarian *et al.* [2014] used a database of 406 laboratory measurements of electrical conductivities of sedimentary rocks in the literature and showed that the relationship between F and porosity was described by percolation scaling in all cases. They found that equation (7) accurately modeled the measured values of F with ϕ_x values between 0.26 and 1. However, they assumed that ϕ_t in all cases was equal to 10% of the porosity value. It is not possible to determine whether their results in some cases are due to the assumption made to determine the percolation threshold. Ghanbarian *et al.* [2014] did include an analysis in their manuscript of F predictions for a set of Bentheimer sandstone samples for which ϕ_t was determined from microtomography images [Berg, 2012] and found that F was best predicted from equation (7) with $\phi_x = 0.93$, which they concluded was reasonably close to a value of 1 to allow percolation scaling up to porosity of 1. Therefore, it is not clear whether effective medium theory (equation (7); bottom line) is necessary to describe any part of the porosity- F relationship. In addition, equation (7) was valid for the samples Ghanbarian *et al.* [2014] considered since they contained negligible clay content and therefore had essentially zero surface conductivity. In what follows we explain how we determined F and ϕ_t for marine clay samples with significant surface conductivity (10–30% of the porewater conductivity).

2.2. Samples

We used data and samples from Ocean Drilling Program (ODP) Leg 190 Sites 1173 and 1174 and Integrated Ocean Drilling Program Expeditions 322 and 333 Sites C0011 and C0012. These sites are located in the Nankai Trough offshore Japan (Figure 1). All four sites are located seaward of the trench on the incoming Philippine Sea Plate; Sites C0011 and C0012 contain undeformed sedimentary inputs to the trench [Underwood *et al.*, 2010], while Sites 1173 and 1174 sampled sediments immediately before and immediately following initiation of strain localization along the décollement, respectively [Shipboard Scientific Party, 2001a]. The sediments at these sites contain hemipelagic sediments of the Upper and Lower Shikoku Basin facies, as well as trench-wedge and trench-to-basin transition facies at Site 1174; lithologies consist of mudstones interbedded with ash, volcanoclastic sands, and turbidites. Clay minerals comprise between 13 and 93 wt % of the sediment matrix, with a mean value of 58% among the four Sites [Shipboard Scientific Party, 2001c, 2001d; Expedition 322 Scientists, 2010b, 2010c; Expedition 333 Scientists, 2012b, 2012c]. The clays are dominantly smectite (35–100% of the clay-size fraction [Steurer and Underwood, 2003; Underwood and Guo, 2013]). Relevant physical property ranges are shown in Table 1.

3. Analytical Techniques

3.1. Electrical Conductivity Measurements

We used electrical conductivities measured shipboard as part of the physical properties workflow at each of the five Sites. In the shallow sections where sediments were sufficiently soft, a four-probe Wenner array was used to measure conductivity. In more lithified sediments, conductivities were measured on discrete cubes with side length ~ 2 cm by placing the cube between two electrodes. In order to compare conductivities measured in the same direction, we only used conductivities in the y direction from the discrete cube measurements since this direction corresponds with the orientation of the current flow of the Wenner array. For more details on the electrical conductivity measurements the reader is referred to Shipboard Scientific Party [2001b], Expedition 322 Scientists [2010a], and Expedition 333 Scientists [2012a].

3.2. Cation Exchange Capacity

Cation exchange capacity (CEC) and exchangeable cation compositions were measured at l'Institut National de la Recherche Agronomique in Arras, France, using cobaltihexamine [Orsini and Remy, 1976]. Exchangeable cation compositions were corrected for pore water contributions using shipboard measurements of interstitial water chemistry [Henry, 1997] assuming that chloride resides only in the free water and not in the bound

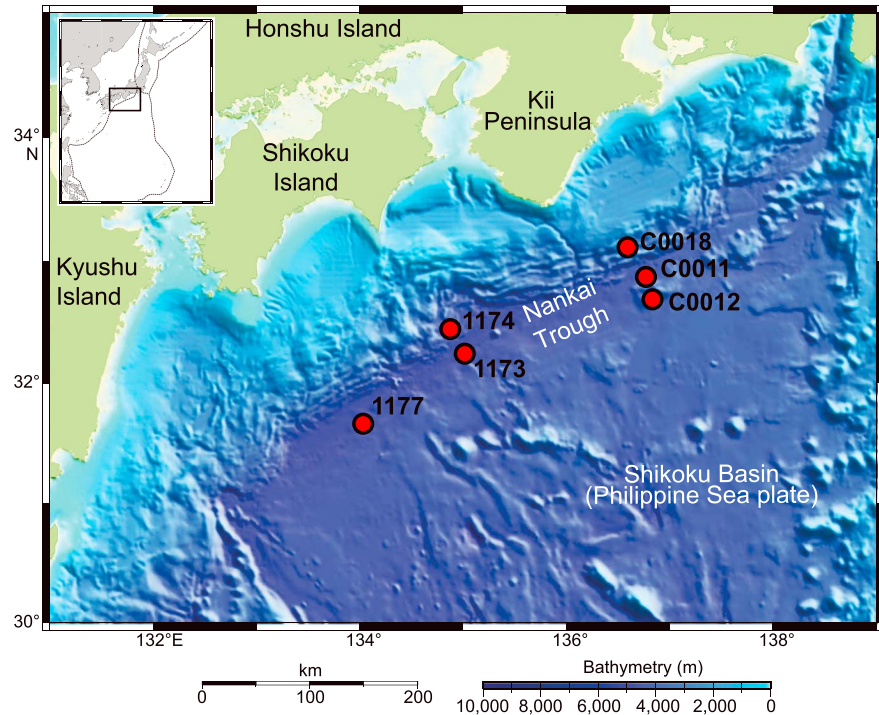


Figure 1. Location of boreholes used in this study in the Nankai Trough offshore Shikoku and Honshu Islands, Japan. Inset shows locations of plate boundaries. The Nankai Trough occurs where the Philippine Sea Plate is being subducted northwestward beneath the Eurasian Plate.

water. Carbonate dissolution that occurred during sample preparation was corrected by assuming that all excess cations remaining after pore water correction were calcium ions. Additional details of the measurements and analysis are given in *Henry and Bourlange [2004]* and *Conin et al. [2011]*. CEC values for Sites C0011 and C0012 are given in Tables S1 and S2 in the supporting information. CEC values for Sites 1173, 1174, and 1177 were previously reported by *Henry and Bourlange [2004]*.

3.3. Dukhin Number and Formation Factor

The Dukhin number ζ was determined as *[Revil et al., 1998]*

$$\zeta = \frac{2\rho_g CEC \beta_s}{3\sigma_f}, \tag{8}$$

where ρ_g is the solid matrix density of the sediment (kg m^{-3}), CEC is the cation exchange capacity (C kg^{-1}), β_s is the equivalent surface mobility for surface electrical conduction ($\text{m}^2 \text{s}^{-1} \text{V}^{-1}$), and σ_f is the conductivity of the pore fluid (S/m). Grain densities were taken from shipboard pycnometer measurements. CEC was converted to C kg^{-1} from mol kg^{-1} using the relationship that 1 mol of equivalent charge = 0.09632 C *[Revil et al., 1998]*. We determined β_s from the cation surface mobilities β_s^i of the exchangeable cations:

$$\beta_s = \frac{\sum_i \beta_s^i Z_i C_i}{\sum_j Z_j C_j}, \tag{9}$$

Table 1. Ranges of Physical Properties for All Samples

CEC (mol kg^{-1})	Porosity	Clay mineral Content (wt %)	Specific Surface ^a ($\text{m}^2 \text{g}^{-1}$)	ϕ_{EDL}	ϕ_t^b	F
0.121–0.665	0.225–0.716	34–89	25.7–77.7	0.052–0.392	0.167–0.533	2.79–28.4

^aSpecific surface = surface area per unit mass of solid matrix. Specific surface values were only available for samples from Sites C0011 and C0012 *[Daigle and Dugan, 2014]*.

^bDetermined as 0.5577ϕ .

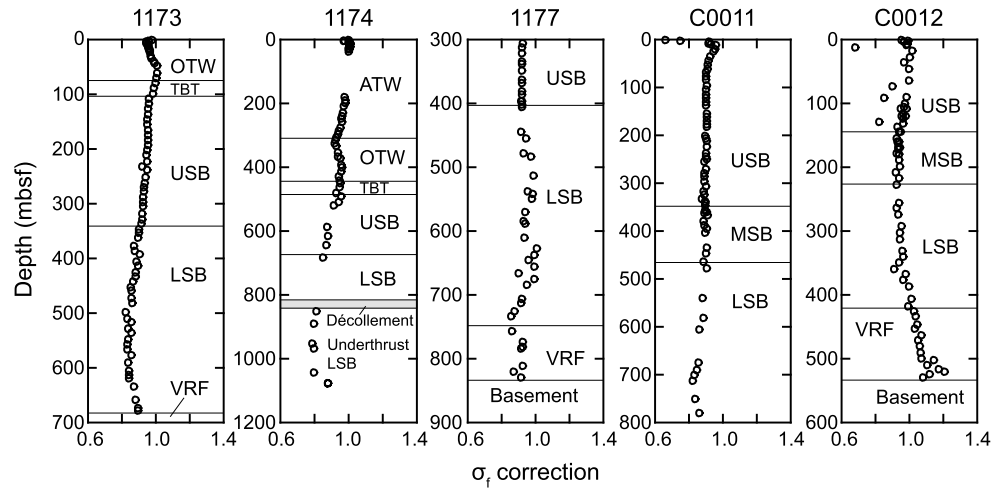


Figure 2. Pore fluid conductivity correction (the ratio on the right-hand side of equation (10)) versus depth (mbsf = meters below seafloor) for each of the 5 Sites considered. Stratigraphy abbreviations: OTW = outer trench wedge, ATW = axial trench wedge, TBT = trench-basin transition, USB = Upper Shikoku Basin facies, MSB = Middle Shikoku Basin facies, LSB = Lower Shikoku Basin facies, VRF = volcanic-rich facies.

where Z_i and C_i are the charges and concentrations (mol kg^{-1}) of the individual cation species [Bourlange et al., 2003]. We determined σ_f from shipboard interstitial water measurements as

$$\sigma_f = \sigma_{f0} \frac{\sum_j \beta_f^j Z_j C_{iws}^j}{\sum_j \beta_f^j Z_j C_{sw}^j}, \tag{10}$$

where β_f^j is the ionic mobility in the pore fluid ($\text{m}^2 \text{s}^{-1} \text{V}^{-1}$), C_{iws}^j is the ionic concentration in the pore fluid (mmol), C_{sw}^j is the ionic concentration in seawater, and σ_{f0} is the conductivity of seawater. Seawater ionic concentrations were determined from International Association for Physical Sciences of the Oceans standard seawater and are given in Table 18 of Expedition 322 Scientists [2010b]. Seawater conductivity was determined as $5.32(1 + 0.02(T - 25))$, where T is the temperature in $^\circ\text{C}$ [Bourlange et al., 2003]. Temperature was taken as the temperature recorded at the time of shipboard conductivity measurement, which was 22–25 $^\circ\text{C}$. Values for β_s^j and β_f^j were taken from Table 1 of Revil et al. [1998]. Because shipboard interstitial water samples were taken at different depths from the CEC measurements, we interpolated the ratio term from equation (10) to determine the pore fluid conductivity correction at the location of each CEC measurement. This correction did not vary substantially between measurement points so the interpolation is not expected to have introduced significant errors (Figure 2). Relevant data for these computations for Sites C0011 and C0012 are given in Tables S3 and S4.

3.4. Threshold Porosity

We assume that ϕ_t in equation (7) represents the ineffective porosity and excludes porosity that does not contribute to flow of electrical current through pore space. We define the ineffective porosity as containing the water in the electrical double layer [e.g., Juhász, 1979; Hill et al., 1979; Peveraro and Thomas, 2010] as well as the pore space outside the electrical double layer that does not percolate [e.g., Koponen et al., 1997; Peveraro and Thomas, 2010]. Our assumption is equivalent to replacing the water in the electrical double layer (Figure 3a) with a solid, nonconducting phase, and allowing the remaining pore space to have a nonzero critical volume fraction ϕ_c (Figure 3b). From the interstitial water data, the ionic strength in all samples we considered was roughly 400 mM. Assuming that the thickness of the electrical double layer in nanometer at room temperature may be estimated from the Debye length as $9.7/l^{0.5}$, where l is the ionic strength in millimole [Russel et al., 1989], the electrical double layers in these samples were on the order of 0.5 nm. This short Debye length suggests that most of the surface charge is countered in the Stern layer and that the mobility of ions in the Stern layer accounts for part of the conductivity [Henry, 1997; Leroy and Revil, 2009; Revil, 2013a, 2013b]. Therefore, we feel that our assumption is valid for the samples we considered.

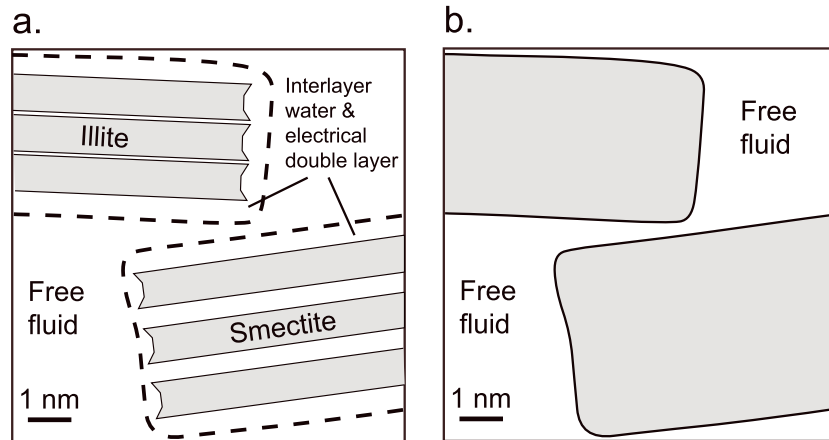


Figure 3. Illustration of our assumptions in determining the threshold porosity. (a) Interlayer water and water in the electrical double layer around clays is replaced with (b) nonconducting, solid material with zero surface conductivity. The remaining pore space in Figure 3b has an associated percolation threshold. Figure modified from *Henry and Bourlange* [2004].

However, at lower ionic strength this assumption will break down. *Bourg and Sposito* [2011] showed that the effective diffusion coefficient of water and dissolved ions exhibit an *e*-fold (i.e., 2.7-fold) decrease from the bulk value within ~1 nm of a smectite surface. Using this as a threshold distance below which ion exchange between the electrical double layer and the bulk pore fluid will not occur, the ionic strength corresponding to this Debye length is roughly 100 mM. For ionic strength less than this value, the electrical double layer may not be considered as a separate, parallel conductive path, and the method used to determine ϕ_t must necessarily consider the contribution of this ionic exchange to the overall conductivity. We additionally caution that in clays, equation (7) is only valid when there is a quantity of pore fluid not associated with the electrical double layer present in a quantity exceeding the percolation threshold. In cases where $\phi < \phi_t$, electrical conduction may still occur through the electrical double layer if it forms a connected phase. This phenomenon has been observed in partially saturated rocks [e.g., *Han et al.*, 2009] as well as low-porosity clays [e.g., *de Lima and Sharma*, 1990]. Conduction is also possible due to Stern layer polarization when measured at nonzero frequencies, particularly between 0.01 Hz and 1 MHz [e.g., *Leroy and Revil*, 2009]. However, in natural porous media the Stern layer does not often form a connected conductive pathway across the sample [*Revil*, 2013a, 2013b]. Our assumptions may not be valid at low porosities when the Stern layer does percolate.

Since ϕ_t represents the ineffective porosity, the quantity $\phi - \phi_t$ therefore is the effective porosity [*Ellis and Singer*, 2007]. We computed the effective porosity in two steps. First, we subtracted the pore volume associated with the electrical double layer, which we show depends on CEC and total porosity. Second, we determined a critical volume fraction for the pore volume from mercury injection capillary pressure (MICP) measurements, since the effective porosity is assumed to refer to the pore volume in excess of the percolation threshold [e.g., *Han et al.*, 2008]. The pore volume remaining after these subtractions was assumed to be the effective porosity.

To determine the volume of fluid in the electrical double layer, we assumed that dissolved chlorides only reside in the free fluid and are excluded from the electrical double layer [e.g., *Clavier et al.*, 1984]. The mass of bound water per unit dry grain mass w_a was determined as [*Henry and Bourlange*, 2004; *Conin et al.*, 2011]

$$w_a = w - \frac{C_s \rho_f}{[Cl^-]}, \tag{11}$$

where w is the total water content of the sediment (mass of water per unit dry grain mass), C_s is the soluble chloride concentration (mol kg^{-1}) determined by sample dilution in deionized water, ρ_f is the density of the pore fluid (taken as 1.024 kg l^{-1}), and $[Cl^-]$ is the pore fluid chloride concentration

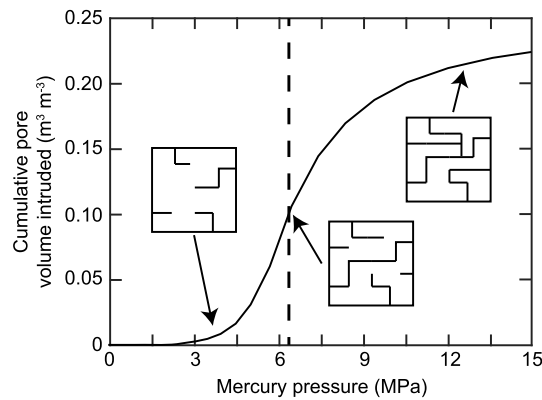


Figure 4. Plot of mercury pressure versus cumulative pore volume intruded for a representative sample from Site C0012 [Daigle and Dugan, 2014]. The cumulative pore volume intruded has been normalized with respect to the porosity exclusive of the volume in the electrical double layer. The line drawings are representative of the pore connections (bonds) occupied by mercury at different points on the curve (after Seaton [1991]), and the percolation threshold is marked by the vertical dashed line. At pore volume less than the percolation threshold, there are no sample-spanning clusters of mercury-filled pores. At the percolation threshold, the first sample-spanning cluster forms, and more connections develop as more mercury is intruded. For this sample we determined $\phi_t = 0.092$.

sample is recorded at each pressure increment. The measurement typically proceeds to a maximum mercury pressure of 55,000 psi (379 MPa). MICP measurements may be used to determine the critical volume fraction, in particular with application to electrical conductivity. Katz and Thompson [1987] showed that the inflection point in a plot of mercury pressure versus cumulative pore volume intruded corresponds to the point at which a sample-spanning electrically conductive pathway forms (Figure 4). Murray et al. [1999] later argued that an MICP measurement is a process analogous to low-pressure nitrogen desorption, which also may be used to determine the percolation threshold [Seaton, 1991; Liu et al., 1992], and that the inflection point in the pressure versus cumulative pore volume defines the percolation threshold. We therefore used MICP measurements to determine the critical volume fraction for samples from Sites C0011 and C0012 [Daigle and Dugan, 2014].

The MICP measurements were not performed at the same depths as the CEC measurements; all MICP measurements were at least 3.19 m away from the nearest CEC measurement at which a ϕ_{EDL} value was determined. Since ϕ_{EDL} is strongly dependent both on total porosity and clay mineral abundance [e.g., Clavier et al., 1984], rather than interpolate between the measured ϕ_{EDL} values we performed a cubic spline interpolation of total porosity and clay mineral abundances determined by X-ray diffraction measurements [Shipboard Scientific Party, 2001c, 2001d, 2001e; Expedition 322 Scientists, 2010b, 2010c; Expedition 333 Scientists, 2012b, 2012c]. The interpolation used a training data set of 75 measurements randomly selected from a total of 99 measurements available from Sites 1173, 1174, 1177, C0011, and C0012. The method fits the remaining 24 measurements with a coefficient of determination (R^2) of 0.822 (Figure 5a). We then determined the critical volume fraction ϕ_c from the mercury pressure versus cumulative volume intruded data; cumulative volume intruded was normalized with respect to the quantity $\phi - \phi_{EDL}$ since we only considered percolation through the pore volume exclusive of the electrical double layer. Finally, we determined ϕ_t as $\phi_t = \phi_{EDL} + \phi_c$.

To allow calculation of ϕ_t at depths corresponding to the CEC measurements, we constructed a regression to compute ϕ_t as a function of ϕ . We assumed a linear relationship with porosity following Bartoli et al. [1999], Hunt [2004], and Ghanbarian et al. [2014]. This resulted in the relationship $\phi_t = 0.5577\phi$, with $R^2 = 0.899$ (Figure 5b). Although this relationship is only strictly valid for sediments of the Shikoku Basin facies with porosity and clay mineral content within certain ranges (0.225–0.716 and 0.34–0.89, respectively) due to the interpolation we used to predict ϕ_{EDL} , it appears to predict ϕ_t well for accretionary prism

(mol l^{-1}) determined from shipboard measurements. We then converted w_a to the porosity associated with the electrical double layer ϕ_{EDL} as

$$\phi_{EDL} = w_a \frac{\rho_g}{\rho_w} (1 - \phi). \quad (12)$$

Porosity in the electrical double layer at Sites C0011 and C0012 is given in Tables S5 and S6. Values for Sites 1173, 1174, and 1177 were previously reported by Henry and Bourlange [2004].

After subtracting ϕ_{EDL} from the total porosity, we determined the critical volume fraction ϕ_c from MICP measurements. During an MICP measurement, an oven-dried sample is evacuated and immersed in mercury. The mercury pressure is then increased stepwise and allowed to stabilize, and the volume of mercury that intrudes the pore space of the

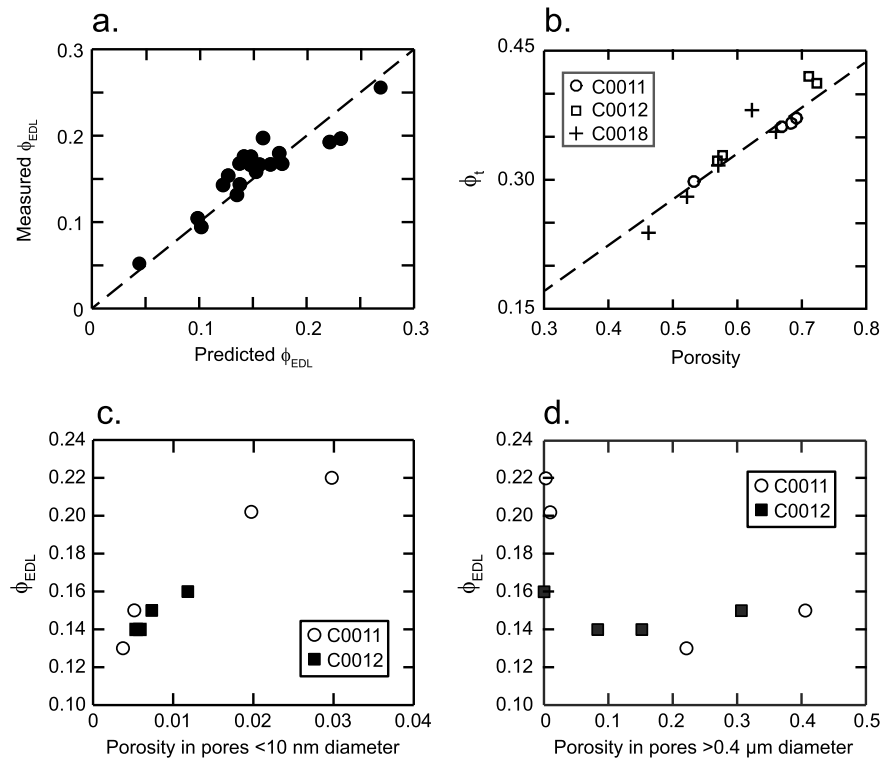


Figure 5. (a) Porosity in the electrical double layer (ϕ_{EDL}) predicted by interpolation plotted against the value determined from CEC measurements for the subset of 24 measurements used as a blind test. Dashed line represents 1:1 equivalence. (b) Threshold porosity determined from MICP measurements versus total porosity. The dashed line is the best fit of $\phi_t = 0.5577\phi$ we determined for the samples from Sites C0011 and C0012. Samples from Site C0018 were not used to determine this fit, yet they lie along the prediction line as well. (c) Relationship between porosity in pores smaller than 10 nm in diameter determined from MICP and porosity in the electrical double layer. (d) Relationship between porosity in pores larger than 0.4 μ m in diameter determined from MICP and porosity in the electrical double layer.

and slope-basin sediments from Site C0018 northwest of Sites C0011 and C0012 (Figure 1), where MICP data were also measured [Daigle and Dugan, 2014] (Figure 5b). This observation strengthens our confidence in this method.

Since much of the water in the electrical double layer is assumed to be gone at the time of MICP measurement due to oven-drying [Ellis and Singer, 2007], we assume that the presence or absence of a layer of bound water surrounding the clay particles will not affect the percolation threshold determined from the MICP measurement and that the collapse of the smectite interlayers due to dehydration only closes the interlayers and does not offset the pore throat size distribution by creating either large pores (such as microcracks) or nanopores within the clay minerals. First, consider the loss of the layer of bound water around the clay particles. The Debye length we determined for our samples (0.5 nm) is small compared to pore widths in these sediments on the order of hundreds of nanometers [Daigle and Dugan, 2014; Dugan, 2015], and the presence or absence of this layer is not expected to have greatly affected the percolation thresholds observed in the MICP measurements. We also note that the addition of a roughly uniform coating to the grain surface would simply rescale the x axis of Figure 4 due to the reciprocal relationship between pore size and capillary pressure, leaving the cumulative pore volume at the inflection point and consequently the critical volume fraction unchanged. Therefore, this effect is not expected to affect the interpretation of the MICP data.

Next, consider the possible change in the pore space brought about by collapse of smectite interlayers. Our assumption that the smectite dehydration process does not strongly affect the pore throat size distribution may be tested by examining the relationship between MICP-derived porosity in pores smaller than 10 nm in diameter and ϕ_{EDL} . The positive relationship between porosity in this size range and ϕ_{EDL} that we observe (Figure 5c) indicates that very small pores associated with clay are either retained or formed during the drying process.

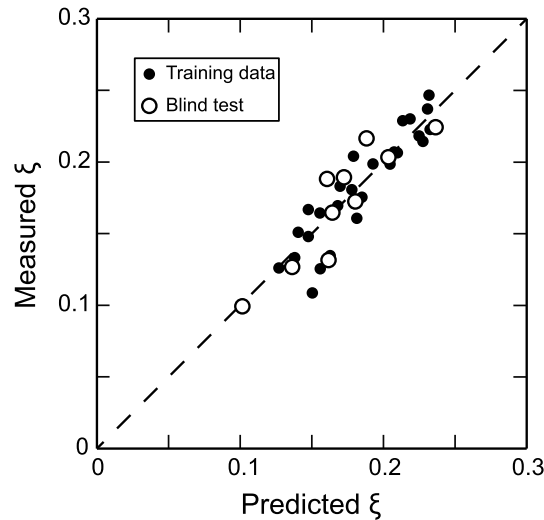


Figure 6. Predicted Dukhin number (ζ) from equation (13) versus measured value determined at Sites C0011 and C0012. The dashed line represents 1:1 equivalence.

However, these nanopores only represent a small fraction of the electrical double layer volume, which indicates that the collapse of the electrical double layer did not strongly affect the lower end of the pore size distribution. Conversely, formation of macropores during smectite dehydration may be assessed by examining correlations of ϕ_{EDL} with the fraction of pores larger than $0.4 \mu\text{m}$. We observe a general lack of such a relationship (Figure 5d), with greater fractions of larger pores generally being associated with less pore volume in the electrical double layer. Therefore, we are confident that the smectite dehydration process only resulted in closure of the smectite interlayers and did not significantly affect the pore size distribution.

We finally note that the small Debye length we determined for our samples does not necessarily mean that ϕ_{EDL} will be small. With clays comprising up to 93 wt % of the sediment matrix [Shipboard Scientific Party, 2001c, 2001d; Expedition 322 Scientists, 2010b, 2010c; Expedition 333 Scientists, 2012b, 2012c] and 35–100% of the clays made up of smectite [Steurer and Underwood, 2003; Underwood and Guo, 2013], most of the bound water is present in clay interlayers. Moreover, the aspect ratio of the individual clay grains is expected to exceed 100 [Santamarina et al., 2002]. The collapse of the interlayers during drying will modify the MICP pore size distribution obtained, shifting it to larger pore sizes, but, as we argued above, this should have little influence on the percolation threshold.

4. Results and Discussion

Because comparing formation factor and effective porosity required comparing data from various measurements that were made at different depths in the boreholes, we used the following scheme to interpolate or assign data. (1) Since the Dukhin number ζ was determined only for a subset of CEC measurements, we used the following empirical relationship to determine ζ for the remaining CEC measurements:

$$\zeta = -0.7166 + 1.504\text{CEC} + 0.003177m_{Na} - 1.187\text{CEC}^2 - 7.867 \times 10^{-4}\text{CEC}m_{Na} - 3.683 \times 10^{-6}m_{Na}^2 \quad (13)$$

where CEC is in mol kg^{-1} and m_{Na} is the concentration of sodium in the interstitial water in mmol. Equation (13) was determined by fitting a training data set of 27 measurements randomly selected from a total of 37 measurements available from Sites C0011 and C0012. The regression fits the remaining 10 measurements with a coefficient of determination (R^2) of 0.799; the R^2 value for the entire data set is 0.824 (Figure 6). (2) Fluid conductivity was determined at each CEC measurement point by interpolating at the CEC measurement depth. (3) Porosity and conductivity were determined from shipboard measurements. We assigned values corresponding to the CEC measurement points by finding the porosity and conductivity measurements that were taken nearest to the CEC measurement along the core. We did no further analysis on CEC measurements that were more than 30 cm away from the nearest porosity or resistivity measurement. (4) We determined ϕ_t from porosity using the regression developed by comparison with the MICP measurements. (5) We determined F from equation (3) using ζ from step 1, σ_w from step 2, and σ from step 3. Therefore, F was only computed at CEC measurement points that were less than 30 cm away from both a porosity and conductivity measurement. In addition, since the relationships used to determine ϕ_t and ζ were determined only on sediments from the Shikoku Basin facies, we restricted our analysis to Shikoku Basin sediments at each Site.

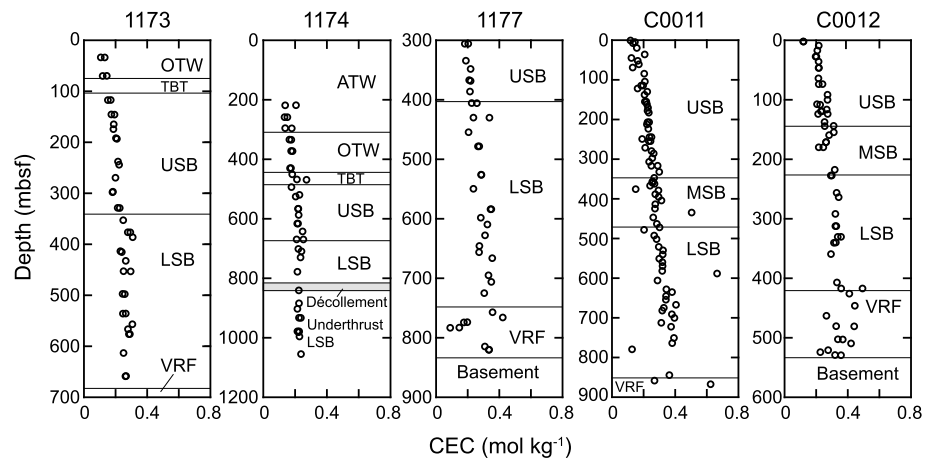


Figure 7. CEC plotted versus depth for each of the five Sites considered. Values for Sites 1173, 1174, and 1177 are from Henry and Bourlange [2004]; values for Sites C0011 and C0012 are from this study. Stratigraphy abbreviations are the same as in Figure 2.

CEC at Sites C0011 and C0012 is shown in Figure 7 with the values at Sites 1173, 1174, and 1177 for reference. Henry and Bourlange [2004] noted that lower CEC values and less scatter in the values in the Lower Shikoku Basin facies at Site 1174 relative to Sites 1173 and 1177 was a consequence of more advanced smectite-to-illite conversion. The higher CEC values in the Lower Shikoku Basin facies and the greater amount of scatter in the values at Sites C0011 and C0012 suggest that very little smectite-to-illite conversion has occurred at these Sites. This is consistent with analyses of clay mineral assemblages at these Sites [Underwood and Guo, 2013]. The Dukhin number generally increases with depth through the Shikoku Basin facies at all five Sites (Figure 8). More advanced smectite-to-illite conversion results in lower Dukhin numbers, as illustrated by Site 1174. This is due to the lower CEC of illite compared to smectite (~0.2 mol kg⁻¹ compared to ~1 mol kg⁻¹ [Patchett, 1975; Lipsicas, 1984; Zundel and Siffert, 1985]). Generally the Dukhin number is >0.1, indicating that surface conductivity is at least 10% of the fluid conductivity in these sediments.

Figure 9 shows F plotted against $\phi - \phi_r$ and a prediction line from equation (7) with $\phi_x = 1$. The scatter about the prediction line exhibited by the data is probably due to the combination of the methods we used to estimate ϕ_{EDL} and ζ and the fact that not all measurements were made at the same depth, despite our restriction to measurements made within 30 cm of each other. However, despite the scatter, it is apparent that all the data are fit well with a crossover porosity of 1; the line in Figure 9 fits the data with $R^2 = 0.809$, which is similar

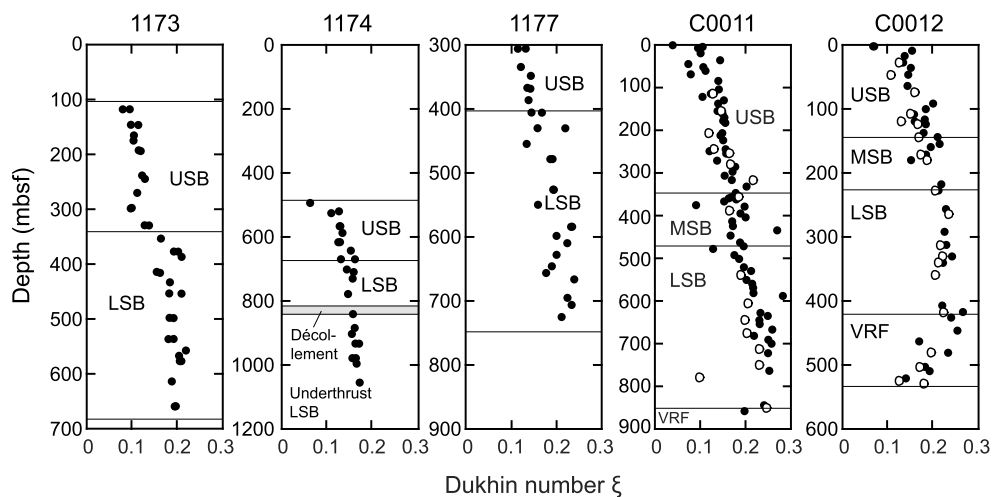


Figure 8. Dukhin number (ζ) versus depth for each of the five Sites considered. Open circles are determinations from CEC measurements; shaded circles are predicted from equation (13). Stratigraphy abbreviations are the same as in Figure 2.

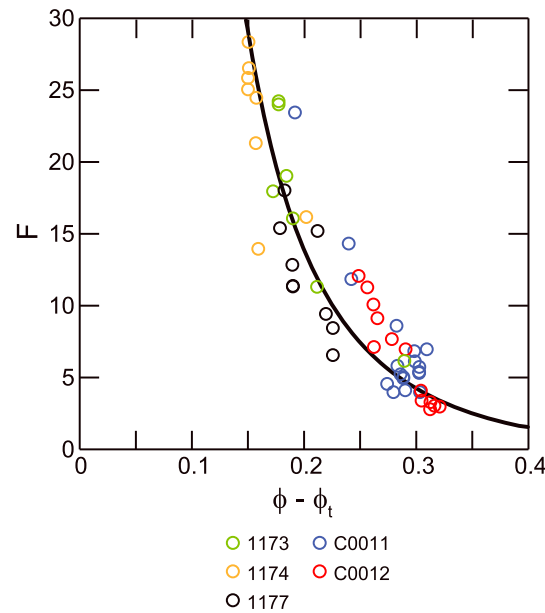


Figure 9. Prediction of formation factor from equation (7). Circles are values determined from laboratory samples. Black line is prediction.

in magnitude to the R^2 values we obtained for the cubic spline interpolation used to determine ϕ_{EDL} and the regression used to determine ζ (equation (12)). Our results indicate that universal scaling from percolation theory applies over the full range of porosities for these samples. Whether this fact is true for clays in general will need to be investigated by future research. Sahimi [1993] suggested that the crossover porosity defining the upper limit of percolation scaling may be approximated in three dimensions as $\phi_x = \phi_t + \phi/Z$, in which Z is the average coordination number (the number of neighboring pores to which a given pore is connected, averaged over all pores). Since we found that $\phi_t = 0.5577\phi$, Sahimi's [1993] expression may be written for our data set as $\phi_x = \phi(0.5577 + 1/Z)$, which may be rearranged to yield $Z = \phi/(1 - 0.5577\phi)$ when $\phi_x = 1$. This expression yields $Z < 1$ when $\phi < 0.642$, which may not be physically realistic for sedimentary rocks since it implies that on average a given pore is not connected to any neighboring pores in rocks with porosity less than 0.642. However, the general implication is that the coordination numbers of these sediments are generally very low, indicating a low degree of connectivity within the pore system. This low connectivity over a wide range of porosities may explain why universal scaling from percolation theory can be applied over the entire porosity range. The condition that percolation scaling is valid only in the vicinity of the percolation threshold may thus be interpreted to imply validity when few sample-spanning clusters are present, either near the percolation threshold in well-connected pore systems or far above the percolation threshold in poorly connected pore systems. In addition, we caution that the universal scaling that we observed may be due to small sample sizes; at the borehole scale or larger, long-range correlations may yield nonuniversal scaling that is still described by percolation theory [Sahimi, 1994b; Sahimi and Mukhopadhyay, 1996].

It is important to note that we considered sediments with nonzero but still small ζ , and our results should be considered in terms of a continuum of ζ values. At $\zeta \approx 0$, F may be expressed as σ_f/σ , and the porosity dependence of F was shown to follow percolation and effective medium scaling by Ghanbarian *et al.* [2014] through analogs with flow through resistor networks. However, considering the general definition of F (equation (1)), it is not obvious that percolation scaling should still apply when ζ is nonnegligible. We have shown that when surface conductivity is 10–30% of the bulk porewater conductivity, F still follows percolation scaling with porosity even though its relationship with the porewater conductivity and overall conductivity of the medium is more complex (equation (3)). The nonnegligible but small surface conductivity allowed us to make several assumptions to determine the percolation threshold. It is not clear whether percolation theory can accurately describe the porosity dependence of F at very large ζ , since the definition of the percolation threshold becomes much more complicated. Further work is necessary to determine the upper limit of ζ at which percolation theory can be used to describe F , or whether a limit exists at all.

5. Conclusions

We presented CEC measurements on samples from IODP Sites C0011 and C0012 in the Nankai Trough. We used these measurements and previously reported data to determine the Dukhin number and formation factor at ODP Sites 1173, 1174, and 1177, and Sites C0011 and C0012. Both the CEC and Dukhin number values appear to be strongly influenced by the degree of smectite-to-illite conversion, with lower values associated with greater amounts of conversion. We compared the formation factor values to predictions from percolation and effective medium theories using scaling relationships previously developed by Ghanbarian *et al.* [2014]. After correcting for the volume of clay-bound water using the CEC measurements and determining

the percolation threshold using a relationship determined from MICP measurements, we found that the scaling relationship expressed in equation (7) accurately predicted the formation factor with $R^2 = 0.809$. Our results suggest that universal scaling from percolation theory is valid over the entire porosity range in these sediments, which is probably due to relatively broad pore size distributions or low connectivity within the pore system. Our work shows that the formation factor follows universal scaling from percolation theory even when significant surface conduction occurs.

Acknowledgments

The data used for this study are available in previously published literature and the supporting information for this manuscript. This research used samples and/or data provided by the Ocean Drilling Program (ODP) and Integrated Ocean Drilling Program (IODP). This work was supported by the University of Texas at Austin. The authors thank the Associate Editor and two anonymous reviewers for their constructive comments that helped strengthen this paper.

References

- Ambegaokar, V., B. Halperin, and J. S. Langer (1971), Hopping conductivity in disordered systems, *Phys. Rev. B*, 4(8), 2612–2620, doi:10.1103/physrevb.4.2612.
- Archie, G. E. (1942), The electrical resistivity log as an aid in determining some reservoir characteristics, *Pet. Trans. AIME*, 146(1), 54–62, doi:10.2118/942054-g.
- Avellaneda, M., and S. Torquato (1991), Rigorous link between fluid permeability, electrical conductivity, and relaxation times for transport in porous media, *Phys. Fluids A*, 3(11), 2529–2540, doi:10.1063/1.858194.
- Bartoli, F., N. R. A. Bird, V. Gomeny, H. Vivier, and S. Niquet (1999), The relation between silty soil structures and their mercury porosimetry curve counterparts: Fractals and percolation, *Eur. J. Soil Sci.*, 50(1), 9–22, doi:10.1046/j.1365-2389.1999.00209.x.
- Berg, C. F. (2012), Re-examining Archie's law: Conductance description by tortuosity and constriction, *Phys. Rev. E*, 86(4), 046314, doi:10.1103/PhysRevE.86.046314.
- Bourg, I. C., and G. Sposito (2011), Molecular dynamics of the electrical double layer on smectite surfaces contacting concentrated mixed electrolyte (NaCl-CaCl₂) solutions, *J. Colloid Interf. Sci.*, 360(2), 701–715, doi:10.1016/j.jcis.2011.04.063.
- Bourlange, S., P. Henry, J. C. Moore, H. Mikada, and A. Klaus (2003), Fracture porosity in the décollement zone of Nankai accretionary wedge using Logging While Drilling resistivity data, *Earth Planet. Sci. Lett.*, 209(1–2), 103–112, doi:10.1016/S0012-821X(03)00082-7.
- Bruggeman, D. A. G. (1935), Berechnung verschiedener physikalischer Konstanten von heterogenen Substanzen I. Dielektrizitätskonstanten und Leitfähigkeiten der Mischkörper aus isotropen Substanzen, *Ann. Phys.*, 416(7), 636–664, doi:10.1002/andp.19354160705.
- Clavier, C., G. Coates, and J. Dumanoir (1984), Theoretical and experimental bases for the dual-water model for interpretation of shaly sands, *Soc. Pet. Eng. J.*, 24(2), 153–168, doi:10.2118/6859-PA.
- Clerc, J. P., V. A. Podolskiy, and A. K. Sarychev (2000), Precise determination of the conductivity exponent of 3D percolation using exact numerical renormalization, *Eur. Phys. J. B*, 15(3), 507–516, doi:10.1007/s100510051153.
- Conin, M., P. Henry, S. Bourlange, H. Raimbourg, and T. Reuschlé (2011), Interpretation of porosity and LWD resistivity from the Nankai accretionary wedge in light of clay physicochemical properties: Evidence for erosion and local overpressuring, *Geochem. Geophys. Geosyst.*, 12, Q0AD07, doi:10.1029/2010GC003381.
- Daigle, H., and B. Dugan (2014), Data report: Permeability, consolidation, stress state, and pore system characteristics of sediments from Sites C0011, C0012, and C0018 of the Nankai Trough, *Proc. Integr. Ocean Drill. Program*, 333, 1–23, doi:10.2204/iodp.proc.333.201.2014.
- de Lima, O. A. L., and M. M. Sharma (1990), A grain conductivity approach to shaly sandstones, *Geophysics*, 55(10), 1347–1356, doi:10.1190/1.1442782.
- Doll, H., R. Sauvage, and M. Martin (1952), Application of micrologging to determination of porosity, *Trans. Gulf Coast Assoc. Geol. Soc.*, 2, 81–106.
- Dugan, B. (2015), Data report: porosity and pore size characteristics of sediments from Site C0002 of the Nankai Trough determined by mercury injection, *Proc. Integr. Ocean Drill. Program*, 338, 1–8, doi:10.2204/iodp.proc.338.202.2015.
- Ellis, D. V., and J. M. Singer (2007), *Well Logging for Earth Scientists*, Springer, Dordrecht, Netherlands.
- Erickson, S. N., and R. D. Jarrard (1998), Porosity/formation-factor relationships for high-porosity siliciclastic sediments from Amazon Fan, *Geophys. Res. Lett.*, 25(13), 2309–2312, doi:10.1029/98GL01777.
- Ewing, R. P., and A. G. Hunt (2006), Dependence of the electrical conductivity in real porous media, *Vadose Zone J.*, 5, 731–741, doi:10.2136/vzj2005.0107.
- Expedition 322 Scientists (2010a), Methods, *Proc. Integr. Ocean Drill. Program*, 322, 1–66, doi:10.2204/iodp.proc.322.102.2010.
- Expedition 322 Scientists (2010b), Site C0011, *Proc. Integr. Ocean Drill. Program*, 322, 1–159, doi:10.2204/iodp.proc.322.103.2010.
- Expedition 322 Scientists (2010c), Site C0012, *Proc. Integr. Ocean Drill. Program*, 322, 1–121, doi:10.2204/iodp.proc.322.104.2010.
- Expedition 333 Scientists (2012a), Methods, *Proc. Integr. Ocean Drill. Program*, 333, 1–50, doi:10.2204/iodp.proc.333.102.2012.
- Expedition 333 Scientists (2012b), Site C0011, *Proc. Integr. Ocean Drill. Program*, 333, 1–96, doi:10.2204/iodp.proc.333.104.2012.
- Expedition 333 Scientists (2012c), Site C0012, *Proc. Integr. Ocean Drill. Program*, 333, 1–93, doi:10.2204/iodp.proc.333.105.2012.
- Ghanbarian, B., and A. G. Hunt (2014), Universal scaling of gas diffusion in porous media, *Water Resour. Res.*, 50, 2242–2256, doi:10.1002/2013WR014790.
- Ghanbarian, B., A. G. Hunt, M. Sahimi, R. P. Ewing, and T. E. Skinner (2013), Percolation theory generates a physically based description of tortuosity in saturated and unsaturated porous media, *Soil Sci. Soc. Am. J.*, 77, 1920–1929, doi:10.2136/sssaj2013.01.0089.
- Ghanbarian, B., A. G. Hunt, R. P. Ewing, and T. E. Skinner (2014), Universal scaling of the formation factor in porous media derived by combining percolation and effective medium theories, *Geophys. Res. Lett.*, 41, 3884–3890, doi:10.1002/2014GL060180.
- Ghanbarian, B., A. G. Hunt, T. E. Skinner, and R. P. Ewing (2015a), Saturation dependence of transport in porous media predicted by percolation and effective medium theories, *Fractals*, 23(1), 1540004, doi:10.1142/S0218348X15400046.
- Ghanbarian, B., H. Daigle, A. G. Hunt, R. P. Ewing, and M. Sahimi (2015b), Gas and solute diffusion in partially saturated porous media: Percolation theory and effective medium approximation compared with lattice Boltzmann simulations, *J. Geophys. Res. Solid Earth*, 120, 189–190, doi:10.1002/2014JB011645.
- Ghanbarian-Alavijeh, B., and A. G. Hunt (2012), Comparison of the predictions of universal scaling of the saturation dependence of the air permeability with experiment, *Water Resour. Res.*, 48, W08513, doi:10.1029/2011WR011758.
- Gingold, D. B., and C. J. Lobb (1990), Percolative conduction in three dimensions, *Phys. Rev. B*, 42(13), 8220–8224, doi:10.1103/PhysRevB.42.8220.
- Halperin, B. I., S. Feng, and P. N. Sen (1985), Differences between lattice and continuum percolation transport exponents, *Phys. Rev. Lett.*, 54(22), 2391–2394, doi:10.1103/PhysRevLett.54.2391.
- Hamamoto, S., P. Moldrup, K. Kawamoto, and T. Komatsu (2010), Excluded-volume expansion of Archie's law for gas and solute diffusivities and electrical and thermal conductivities in variably saturated porous media, *Water Resour. Res.*, 46, W06514, doi:10.1029/2009WR008424.
- Han, H., D. Giménez, and A. Lilly (2008), Textural averages of saturated soil hydraulic conductivity predicted from water retention data, *Geoderma*, 146(1–2), 121–128, doi:10.1016/j.geoderma.2008.05.017.

- Han, M., S. Youssef, E. Rosenberg, M. Fleury, and P. Levitz (2009), Deviation from Archie's law in partially saturated porous media: Wetting film versus disconnectedness of the conducting phase, *Phys. Rev. E*, *79*(3), 031127, doi:10.1103/physreve.79.031127.
- Henry, P. (1997), Relationship between porosity, electrical conductivity, and cation exchange capacity in Barbados wedge sediments, *Proc. Ocean Drill. Program Sci. Results*, *156*, 137–150, doi:10.2973/odp.proc.sr.156.020.1997.
- Henry, P., and S. Bourlange (2004), Smectite and fluid budget at Nankai ODP sites derived from cation exchange capacity, *Earth Planet. Sci. Lett.*, *219*(1–2), 129–145, doi:10.1016/S0012-821X(03)00694-0.
- Hill, H. J., O. J. Shirley, G. E. Klein, M. H. Waxman, and E. C. Thomas (1979), Bound water in shaly sands – Its relation to Q_v and other formation properties, *Log Anal.*, *20*(3), 3–19.
- Hunt, A. G. (2004), Percolative transport in fractal porous media, *Chaos Soliton. Fract.*, *19*(2), 309–325, doi:10.1016/s0960-0779(03)00044-4.
- Hunt, A., R. Ewing, and B. Ghanbarian (2014a), *Percolation Theory for Flow in Porous Media*, 3rd ed., Springer, Dordrecht, Netherlands.
- Hunt, A., B. Ghanbarian, and R. P. Ewing (2014b), Saturation dependence of solute diffusion in porous media: Universal scaling compared with experiments, *Vadose Zone J.*, *13*(4), doi:10.2136/vzj2013.08.0204.
- Johnson, D. L., T. J. Plona, and H. Kojima (1986), Probing porous media with 1st sound, 2nd sound, 4th sound, and 3rd sound, *AIP Conf. Proc.*, *154*, 243–277, doi:10.1063/1.36398.
- Juhász, I. (1979), The central role of Q_v and formation-water salinity in the evaluation of shaly formations, *Log Anal.*, *20*(4), 3–13.
- Katz, A. J., and A. H. Thompson (1986), Quantitative prediction of permeability in porous rock, *Phys. Rev. B*, *34*(11), 8179–8181, doi:10.1103/physrevb.34.8179.
- Katz, A. J., and A. H. Thompson (1987), Prediction of rock electrical conductivity from mercury injection measurements, *J. Geophys. Res.*, *92*(B1), 599–607, doi:10.1029/JB092ib01p00599.
- Kennedy, W. D., and D. C. Herrick (2012), Conductivity models for Archie rocks, *Geophysics*, *77*(3), WA109–WA128, doi:10.1190/geo2011-0297.1.
- Kermabon, A., C. Gehin, and P. Blavier (1969), A deep-sea electrical resistivity probe for measuring porosity and density of unconsolidated sediments, *Geophysics*, *34*(4), 554–571, doi:10.1190/1.1440031.
- Kiefer, T., G. Villanueva, and J. Brugger (2009), Conduction in rectangular quasi-one-dimensional and two-dimensional random resistor networks away from the percolation threshold, *Phys. Rev. E*, *80*, 21104, doi:10.1103/PhysRevE.80.21104.
- Kirkpatrick, S. (1971), Classical transport in disordered media: Scaling and effective-medium theories, *Phys. Rev. Lett.*, *27*(25), 1722–1725, doi:10.1103/physrevlett.27.1722.
- Kirkpatrick, S. (1973), Percolation and conduction, *Rev. Mod. Phys.*, *45*(4), 574–588, doi:10.1103/revmodphys.45.574.
- Knackstedt, M. A., S. J. Marrink, A. P. Sheppard, W. V. Pinczewski, and M. Sahimi (2001), Invasion percolation on correlated and elongated lattices: Implications for the interpretation of residual saturations in rock cores, *Transport Porous Med.*, *44*(3), 465–485, doi:10.1023/A:1010770010309.
- Koponen, A., M. Kataja, and J. Timonen (1997), Permeability and effective porosity of porous media, *Phys. Rev. E*, *56*(3), 3319–3325, doi:10.1103/PhysRevE.56.3319.
- Leroy, P., and A. Revil (2009), A mechanistic model for the spectral induced polarization of clay materials, *J. Geophys. Res.*, *114*, B10202, doi:10.1029/2008JB006114.
- Lipsicas, M. (1984), Molecular and surface interactions in clay intercalates, in *Physics and Chemistry of Porous Media*, edited by D. L. Johnson and P. N. Sen, pp. 191–202, Am. Inst. of Phys., New York, doi:10.1063/1.34298.
- Liu, H., L. Zhang, and N. A. Seaton (1992), Determination of the connectivity of porous solids from nitrogen sorption measurements – II. Generalisation, *Chem. Eng. Sci.*, *47*(17/18), 4393–4404, doi:10.1016/0009-2509(92)85117-t.
- Lyklema, J. (1993), *Fundamentals of Interface and Colloid Science*, vol. 1, Academic Press, London, U. K.
- Mendelson, K. S., and M. H. Cohen (1982), The effect of grain anisotropy on the electrical properties of sedimentary rocks, *Geophysics*, *47*(2), 257–263, doi:10.1190/1.1441332.
- Murray, K. L., N. A. Seaton, and M. A. Day (1999), Use of mercury intrusion data, combined with nitrogen adsorption measurements, as a probe of pore network connectivity, *Langmuir*, *15*(23), 8155–8160, doi:10.1021/la990250x.
- Orsini, L., and J.-C. Remy (1976), Utilisation du chlorure de cobaltihexamine pour la détermination simultanée de la capacité d'échange et des bases échangeables des sols, *Sci. Sol.*, *4*, 269–275.
- Patchett, J. G. (1975), An investigation of shale conductivity, paper presented at SPWLA 16th Annual Logging Symposium, Soc. of Prof. Well Log Anal., paper U, New Orleans, LA.
- Pevararo, R., and E. C. Thomas (2010), Effective porosity: A defensible definition for shaly sands, paper presented at SPWLA 51st Annual Logging Symposium, Soc. of Prof. Well Log Anal., paper 97677, Perth, Australia.
- Revil, A. (2013a), Effective conductivity and permittivity of unsaturated porous materials in the frequency range 1 mHz–1 GHz, *Water Resour. Res.*, *49*, 306–327, doi:10.1029/2012WR012700.
- Revil, A. (2013b), On charge accumulation in heterogeneous porous rocks under the influence of an external electric field, *Geophysics*, *78*(4), D271–D291, doi:10.1190/geo2012-0503.1.
- Revil, A., and P. W. J. Glover (1997), Theory of ionic-surface electrical conduction in porous media, *Phys. Rev. B*, *55*(3), 1757–1773, doi:10.1103/PhysRevB.55.1757.
- Revil, A., L. M. Cathles III, S. Losh, and J. A. Nunn (1998), Electrical conductivity in shaly sands with geophysical applications, *J. Geophys. Res.*, *103*(B10), 23,925–23,936, doi:10.1029/98JB02125.
- Revil, A., P. Kessouri, and C. Torres-Verdin (2014), Electrical conductivity, induced polarization, and permeability of the Fontainebleau sandstone, *Geophysics*, *79*(5), D301–D318, doi:10.1190/geo2014-0036.1.
- Russel, W. B., D. A. Saville, and W. R. Schowalter (1989), *Colloidal Dispersions*, 1st ed., Cambridge Univ. Press, Cambridge, U. K.
- Sahimi, M. (1993), Fractal and superdiffusive transport and hydrodynamic dispersion in heterogeneous porous media, *Transport Porous Med.*, *13*(1), 3–40, doi:10.1007/bf00613269.
- Sahimi, M. (1994a), Long-range correlated percolation and flow and transport in heterogeneous porous media, *J. Phys. I*, *4*, 1263–1268, doi:10.1051/jp1:1994107.
- Sahimi, M. (1994b), *Applications of Percolation Theory*, Taylor and Francis, London, U. K.
- Sahimi, M. (2003), *Heterogeneous Materials II. Nonlinear and Breakdown Properties and Atomistic Modeling*, Springer, Dordrecht, Netherlands.
- Sahimi, M. (2011), *Flow and Transport in Porous Media and Fractured Rock: From Classical Methods to Modern Approaches*, Wiley-VCH, Weinheim, Germany.
- Sahimi, M., and S. Mukhopadhyay (1996), Scaling properties of a percolation model with long-range correlations, *Phys. Rev. E*, *54*(4), 3870, doi:10.1103/PhysRevE.54.3870.
- Sahimi, M., L. E. Scriven, and H. T. Davis (1984), On the improvement of the effective-medium approximation to the percolation conductivity problem, *J. Phys. C Solid State*, *17*(11), 1941–1948, doi:10.1088/0022-3719/17/11/013.

- Sali, L., and D. J. Bergman (1997), Effective medium approximation for strongly nonlinear media, *J. Stat. Phys.*, *86*(3/4), 455–479, doi:10.1007/BF02199110.
- Santamarina, J. C., K. A. Klein, Y. H. Wang, and E. Prencke (2002), Specific surface: Determination and relevance, *Can. Geotech. J.*, *39*(1), 233–241, doi:10.1139/T01-077.
- Seaton, N. A. (1991), Determination of the connectivity of porous solids from nitrogen sorption measurements, *Chem. Eng. Sci.*, *46*(8), 1895–1909, doi:10.1016/0009-2509(91)80151-n.
- Sen, P. N., C. Scala, and M. H. Cohen (1981), A self-similar model for sedimentary rocks with application to the dielectric constant of fused glass beads, *Geophysics*, *46*(5), 781–795, doi:10.1190/1.1441215.
- Shipboard Scientific Party (2001a), Leg 190 summary, *Proc. Ocean Drill. Program Initial Rep.*, *190*, 1–87, doi:10.2973/odp.proc.ir.190.101.2001.
- Shipboard Scientific Party (2001b), Explanatory notes, *Proc. Ocean Drill. Program Initial Rep.*, *190*, 1–51, doi:10.2973/odp.proc.ir.190.103.2001.
- Shipboard Scientific Party (2001c), Site 1173, *Proc. Ocean Drill. Program Initial Rep.*, *190*, 1–147, doi:10.2973/odp.proc.ir.190.104.2001.
- Shipboard Scientific Party (2001d), Site 1174, *Proc. Ocean Drill. Program Initial Rep.*, *190*, 1–149, doi:10.2973/odp.proc.ir.190.105.2001.
- Shipboard Scientific Party (2001e), Site 1177, *Proc. Ocean Drill. Program Initial Rep.*, *190*, 1–91, doi:10.2973/odp.proc.ir.190.108.2001.
- Skaggs, T. H. (2011), Assessment of critical path analyses of the relationship between permeability and electrical conductivity of pore networks, *Adv. Water Resour.*, *34*(10), 1335–1342, doi:10.1016/j.advwatres.2011.06.010.
- Stauffer, D., and A. Aharony (1992), *Introduction to Percolation Theory*, 2nd ed., Taylor and Francis, London, U. K.
- Steurer, J. F., and M. B. Underwood (2003), Clay mineralogy of mudstones from the Nankai Trough reference Sites 1173 and 1177 and frontal accretionary prism Site 1174, *Proc. Ocean Drill. Program Sci. Results*, *190/196*, 1–37, doi:10.2973/odp.proc.sr.190196.211.2003.
- Torquato, S., and S. Hyun (2001), Effective-medium approximation for composite media: Realizable single-scale dispersions, *J. Appl. Phys.*, *89*(3), 1725–1729, doi:10.1063/1.1336523.
- Turban, L. (1978), On the effective-medium approximation for bond-percolation conductivity, *J. Phys. C Solid State*, *11*(3), 449–459, doi:10.1088/0022-3719/11/3/008.
- Underwood, M. B., and J. Guo (2013), Data report: Clay mineral assemblages in the Shikoku Basin, NanTroSEIZE subduction inputs, IODP Sites C0011 and C0012, *Proc. Integr. Ocean Drill. Program*, *322*, 1–34, doi:10.2973/iodp.proc.322.202.2013.
- Underwood, M. B., S. Saito, Y. Kubo, and the Expedition 322 Scientists (2010), Expedition 322 summary, *Proc. Integr. Ocean Drill. Program*, *322*, 1–60, doi:10.2204/iodp.proc.322.101.2010.
- Waxman, M. H., and L. J. M. Smits (1968), Electrical conductivities in oil-bearing shaly sands, *Soc. Pet. Eng. J.*, *8*(2), 107–122, doi:10.2118/1863-A.
- Zundel, J. P., and B. Siffert (1985), Mécanisme de rétention de l'octylbenzene sulfonate de sodium sur les minéraux argileux, in *Solid-liquid Interactions in Porous Media*, pp. 447–462, Technip, Paris.